



HAL
open science

Grid turbulence near the grid

Wouter J.T. Bos

► **To cite this version:**

| Wouter J.T. Bos. Grid turbulence near the grid. 2019. hal-02063500v1

HAL Id: hal-02063500

<https://hal.science/hal-02063500v1>

Preprint submitted on 11 Mar 2019 (v1), last revised 19 Oct 2020 (v2)

HAL is a multi-disciplinary open access archive for the deposit and dissemination of scientific research documents, whether they are published or not. The documents may come from teaching and research institutions in France or abroad, or from public or private research centers.

L'archive ouverte pluridisciplinaire **HAL**, est destinée au dépôt et à la diffusion de documents scientifiques de niveau recherche, publiés ou non, émanant des établissements d'enseignement et de recherche français ou étrangers, des laboratoires publics ou privés.

Grid turbulence near the grid

By **Wouter J. T. BOS**,

LMFA-CNRS, Ecole Centrale de Lyon, Université de Lyon, Ecully, France

(Received 2019)

In grid turbulence, not so far behind the grid, an average flow can be observed with a close to sinusoidal velocity profile, corresponding to the wakes behind the grid bars. The kinetic energy of this mean flow decays rapidly and a close to isotropic flow is observed further downstream. We show how these wakes behind the grid-bars influence the down-stream turbulence. In particular, we investigate the decay rate of kinetic energy, the behavior of the normalized dissipation rate, and the sensitivity of the flow on initial conditions. We show that the initial value of the ratio of the lengthscale of the turbulence to the mesh-size determines the precise decay of the mean-flow and the generation of the turbulent kinetic energy. We further show how a simple turbulence model can estimate the degree of non-equilibrium of a flow.

1. Introduction

Since the first experiments of Simmons & Salter, 1934 (see also ref. Taylor, 1935), the turbulent motion behind a grid in a wind-tunnel has been investigated intensively in a large number of experiments. The main reason is that this type of flow is experimentally close to the academic reference case of isotropic turbulence. Historically, grid-turbulence experiments were therefore carried out avoiding systematically the region close to the grid, where a non-isotropic and inhomogeneous production of kinetic energy by shear-layers behind the grid bars is present. For instance, in early work (Batchelor & Townsend, 1948) it was mentioned: "*The range $x/M < 20$ is of course excluded from the system of classification since the turbulence takes a little time to become uniform (in the lateral direction) and isotropic.*". M is here the mesh-size, and x the distance from the grid in the streamwise direction. Consequently, most studies on grid-turbulence investigated this far downstream evolution (see e.g., Mohamed & Larue, 1990, Mydlarski & Warhaft, 1996).

However, in recent work, reviewed in Vassilicos, 2015, it was recognized that this zone, closer to the grid might be of interest, since it allows the investigation of a transition region between a flow where production and dissipation are both important, and a freely decaying, productionless flow further downstream. In this region several interesting observations were made which were not in complete agreement with classical pictures of self-similar decaying turbulence (e.g., Tennekes & Lumley, 1972). Since then, critical assessment by simulations and experiments of decaying grid-turbulence closer to the grid has opened the debate of the nature of this non-equilibrium turbulence and its dependence on the grid-type (Krogstad & Davidson, 2011, Nagata *et al.*, 2013, Discetti *et al.*, 2013, Thormann & Meneveau, 2014).

One of the observations in the recent grid turbulence experiments (Vassilicos, 2015) is that the normalized dissipation rate is not constant in the near grid region. The

normalized dissipation rate is defined by

$$C_\epsilon = \frac{\epsilon \mathcal{L}}{\mathcal{U}^3}, \quad (1.1)$$

with \mathcal{L} the integral lengthscale, ϵ the dissipation of kinetic energy and \mathcal{U} the RMS velocity fluctuation. In a recent work we explained some of the observations using a perturbation analysis of the energy flux around an equilibrium state (Bos & Rubinstein, 2017). However, a full picture, including the influence of the shear layers on the turbulence production and their influence on the decay rate of the turbulent kinetic energy further downstream has not been given yet, except from a tentative study using the EDQNM turbulence model (Meldi & Sagaut, 2018). The goal of the present investigation is to understand this transition zone, close to the grid for the case of high-Reynolds number turbulence. We will show how the kinetic energy of the turbulence is produced by the shear layers, and how the kinetic energy evolves as a function of time.

This investigation will show that several salient features of near grid-turbulence, as observed in recent investigations can be reproduced by one of the simplest existing turbulence models. In particular, we shall answer to several of the standing questions, as summarized in the list of future issues, which was dressed in Vassilicos, 2015:

- What causes the sudden transition from the power law evolution of C_ϵ to an (almost) constant value,
- What is the downstream distance where this happens?
- How can this downstream distance be estimated in terms of the geometry of the turbulence generator and inlet Reynolds number?

In addition, we will answer to the questions:

- How relates the peak of the kinetic energy to the total kinetic energy injected in the flow?
- How depends the peak of the kinetic energy and its downstream distance from the grid on the flow properties.

We can summarize our main objective in one question: how does grid-turbulence depend on initial conditions?

In section 2 we will show how the mean-field behind the grid-bars can be described in a simple manner. This mean-field loses its energy to the turbulent fluctuations, and this interaction is described and modeled in section 3. In section 4 we show how non-equilibrium can be assessed within a two-equation turbulence model. The model which describes the interaction of the averaged grid-wakes and the turbulent fluctuations is numerically integrated in section 5 for experimentally relevant parameters. These results allow to answer the above stated open questions, which are replied on in the conclusions, section 6.

2. A simplified description of the mean flow

In the present work we will decompose grid-generated turbulence into a mean part (the wakes behind the grid-bars) and a fluctuating part (Reynolds, 1895), and we will investigate how the interaction between the energy in these two components of the flow is influenced by initial conditions.

The mean flow indicated by \bar{U}_i is assumed unidirectional (in the streamwise (x) direction) and varies in the cross-stream (y) direction. Obviously there are two cross-stream directions in the flow behind a regular square-grid, but given the further approximations we introduce, considering one direction is a fine enough description. We will measure the velocity-field in the frame of reference moving with the wind-tunnel average speed U_0 , so

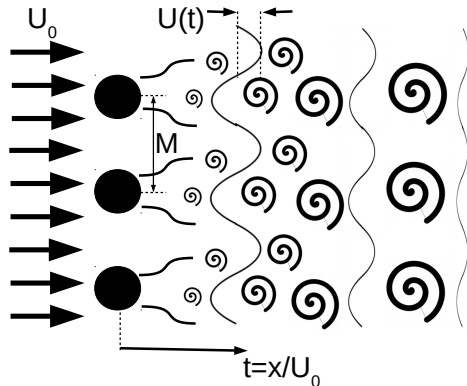


FIGURE 1. Sketch of the geometry considered in the present investigation. A uniform incoming flow $U_0 \mathbf{e}_x$ is perturbed by a grid. The resulting flow is decomposed into a sinusoidal mean profile $U(y) = \bar{U}_x - U_0$ and a fluctuating part.

that the mean-flow \bar{U}_i is zero when averaged over the cross-stream direction. A sketch of the flow is given in figure 1.

The mean-flow is thus given by

$$\bar{\mathbf{U}}(\mathbf{x}, t) = \bar{U}(y, t) \mathbf{e}_x. \quad (2.1)$$

We now consider the case of regularly spaced grid-bars as used in the majority of studies on grid-turbulence. The spacing of the bars is M (the mesh length). The mean flow behind the bars will then be periodic with a spatial period M . To some approximation we can then model the mean flow by

$$\bar{U}(y, t) = U(t) \cos\left(\frac{2\pi y}{M}\right). \quad (2.2)$$

This can be shown to be a good approximation even for more complicated passive turbulence-generating grids (Valente & Vassilicos, 2014). Indeed, behind fractal grids the wakes were also shown to rapidly converge to a sine-like shape. We anticipate that in active-grids, where a larger transverse turbulent diffusion is generated, the sine-like profiles are probably less prominent. We will come back to this issue later.

By prescribing the shape of the mean-flow, we have simplified the problem considerably. It will now be possible to describe the interaction of the mean flow with the fluctuating turbulent field in a fairly simple manner. We consider the kinetic energy of the mean field, averaged over one mesh length,

$$K = \frac{1}{M} \int_0^M \frac{1}{2} \bar{U}(y, t)^2 dy = \frac{1}{4} U(t)^2. \quad (2.3)$$

The evolution of this quantity is simply derived from the Reynolds averaged Navier-Stokes equations (see appendix 1),

$$\dot{K} = -p - D \quad (2.4)$$

where

$$p = -\frac{1}{M} \int_0^M \overline{uv} \partial_y \bar{U} dy, \quad (2.5)$$

and

$$D = \frac{1}{M} \int_0^M \nu (\partial_y \bar{U})^2 dy, \quad (2.6)$$

with $\bar{u}\bar{v}$ the Reynolds stress. The contribution of the turbulent diffusion in the cross-stream direction vanishes in the energy balance since its integral over a period M is zero (see appendix 1, where we derive this average balance from the pointwise evolution equations).

The fluctuating part of the turbulence, i.e., the turbulent flow that is studied in most investigations of grid-turbulence, is governed by the balance (see appendix 1)

$$\dot{k} = p - \epsilon, \quad (2.7)$$

where

$$k = \frac{1}{M} \int_0^M \frac{1}{2} \overline{u_i u_i} dy. \quad (2.8)$$

and

$$\epsilon = \frac{1}{M} \int_0^M \overline{\nu \partial_j u_i \partial_j u_i} dy. \quad (2.9)$$

where k and ϵ are the kinetic energy and dissipation rate of kinetic energy, both averaged over a grid-period. We have therefore at this point a flow-field, described by the two quantities k and K , and their equations contain the unknown terms $\bar{u}\bar{v}$ and ϵ . We note that the formulation is in particular simple because we consider the kinetic energy budgets averaged over a grid-period, and not pointwise (see appendix 1), so that the turbulent diffusion terms vanish. This simplification is no approximation, but a consequence of the periodicity of the flow. To proceed we need to introduce a model.

3. Modeling the turbulence production

The most widely known turbulence model is the k - ϵ model (Jones & Launder, 1972). To describe the turbulence, equations are written for the quantities k and ϵ . In addition to its simplicity, it is known to give good results both in self-similar decaying turbulence and in shear-flows, even though some precise quantitative features are mispredicted (Pope, 2000). Since we consider the transition zone between a simple shear-flow and a freely decaying flow, the k - ϵ model seems to be the ideal starting point of our investigation.

The k - ϵ model is an eddy-viscosity closure, where the Reynolds stresses are modeled by

$$\bar{u}\bar{v} = -\nu_T \partial_y \bar{U}. \quad (3.1)$$

The eddy viscosity ν_T is modeled as a function of k and ϵ ,

$$\nu_T = C_\nu \frac{k^2}{\epsilon}. \quad (3.2)$$

The kinetic energy of the mean flow (constituted by the shearlayers behind the grid) is determined by relation (2.4). The k - ϵ equations reduce in our description to expression (2.7) for the turbulent kinetic energy and the ϵ -equation,

$$\dot{\epsilon} = \frac{\epsilon}{k} (C_{\epsilon 1} p - C_{\epsilon 2} \epsilon) \quad (3.3)$$

with

$$p = C_\nu \frac{k^2}{\epsilon} \frac{1}{M} \int_0^M (\partial_y \bar{U})^2 dy. \quad (3.4)$$

In order to close the system, we need to determine the average squared shear which appears in expressions (2.6) and (3.4) for D and p , respectively. We can obtain this quantity exactly by averaging the squared gradient of the mean velocity profile given by (2.2) over the y direction,

$$\begin{aligned} \frac{1}{M} \int_0^M (\partial_y \bar{U})^2 dy &= \frac{2\pi^2}{M^2} U^2 \\ &= \frac{8\pi^2}{M^2} K. \end{aligned} \quad (3.5)$$

Thereby, we have reduced our problem to the three ODEs,

$$\dot{K} = -\frac{k^2}{\epsilon} \frac{K}{\tilde{M}^2} \left(1 + \frac{C_\nu}{Re} \right) \quad (3.6)$$

$$\dot{k} = \frac{k^2}{\epsilon} \frac{K}{\tilde{M}^2} - \epsilon \quad (3.7)$$

$$\dot{\epsilon} = \frac{\epsilon}{k} \left(C_{\epsilon 1} \frac{k^2}{\epsilon} \frac{K}{\tilde{M}^2} - C_{\epsilon 2} \epsilon \right), \quad (3.8)$$

where $\tilde{M} = M/(\sqrt{8C_\nu}\pi)$ and $Re = k^2/(\epsilon\nu)$. In the following we will consider the high Reynolds number case, where the last term in brackets of equation (3.6) is negligible. Evidently, since k and ϵ are positive quantities, all quantities will eventually decay. We have therefore an initial value problem depending on the values of K , M , k and ϵ . Since we consider the high Reynolds number case, the viscosity does not enter the system.

Further insights into this system are obtained by rewriting the equations of k and ϵ in their original form, and the equation of the mean-field as an equation for p

$$\frac{\dot{k}}{k} = \frac{\epsilon}{k} \left(\frac{p}{\epsilon} - 1 \right) \quad (3.9)$$

$$\frac{\dot{\epsilon}}{\epsilon} = \frac{\epsilon}{k} \left(C_{\epsilon 1} \frac{p}{\epsilon} - C_{\epsilon 2} \right) \quad (3.10)$$

$$\frac{\dot{p}}{p} = \frac{\epsilon}{k} \left((2 - C_{\epsilon 1}) \frac{p}{\epsilon} - (2 - C_{\epsilon 2}) - \frac{k^3}{\epsilon^2 \tilde{M}^2} \right). \quad (3.11)$$

A salient feature of this representation is that, apart from k, p, ϵ , the dynamics of the production depend explicitly on the square of a lengthscale ratio,

$$\alpha_L(t) \equiv \frac{k(t)^{3/2}}{\epsilon(t)} \frac{1}{\tilde{M}} \sim \frac{L(t)}{M}. \quad (3.12)$$

where we introduce a lengthscale $L \sim k^{(3/2)}/\epsilon$, characterizing the turbulence. For given values of k, p, ϵ , the dynamics can thus be different depending on the initial value of α_L . Clearly, this term in the equations shows how the initial conditions explicitly affect the decay of grid turbulence. We note here that in the experiments (Vassilicos, 2015), it is also a ratio of a local parameter and a parameter linked to the initial conditions which pilots the behaviour of the turbulence. A similar observation was made in Meldi & Sagaut, 2018, who identified a timescale ratio which quantifies the influence of the initial conditions. We note in this context that α_L^2 can also be interpreted as a timescale ratio, and we will come back to this in section 5.4.

It has long been argued that initial conditions might influence a freely evolving turbulent flow for a long time (George, 1992). The present description shows how this influence shows up in the evolution equations of the turbulent kinetic energy. In real experiments

a drastic way to increase the initial value of this parameter is to use active grids (Makita, 1991). Indeed, in active grids the typical lengthscale of the turbulence is largely increased, since instead of developing gradually from instabilities in the grid-wakes, the turbulent kinetic energy is immediately generated by the grid, at the expense of the energy of the mean wake-flow. In the present investigation, in order to illustrate the importance of the initial conditions on the turbulence, we will assess the influence of α_L on the downstream turbulence.

4. Non-equilibrium scaling of unsteady turbulence

In the absence of production, the $k - \epsilon$ model depends only on two parameters, k and ϵ . Therefore, the turbulence is represented by a single lengthscale, determined by relation (1.1), or equivalently, a single timescale k/ϵ . In unsteady flows, another timescale can be defined, determined by the time-variation of the dissipation rate,

$$\tau_\epsilon = \left(\frac{\dot{\epsilon}}{\epsilon} \right)^{-1}. \quad (4.1)$$

It is this second timescale which becomes important when there is a significant imbalance between production and dissipation.

In our recent theory (Bos & Rubinstein, 2017) we acknowledged the importance of this second timescale in the description of unsteady turbulence. We decomposed a turbulent flow into an equilibrium part, consisting in the turbulence which would result when an equilibrium is established between production and dissipation ($p - \epsilon = 0$), and the remaining, disequilibrium part \tilde{k} . In the equilibrium part of the flow, the normalized dissipation (expression (1.1)) yields a constant value $C_{\epsilon 0}$.

We found for the ideal case of high Reynolds number isotropic turbulence a relation between the equilibrium and non-equilibrium parts, given by

$$\frac{\tilde{k}}{k} = \frac{2 \dot{\epsilon} k}{9 \epsilon^2}. \quad (4.2)$$

Since this relation depends on $\dot{\epsilon}$, for which the $k - \epsilon$ model gives an expression [equation (3.3)], we find that

$$\frac{\tilde{k}}{k} = \frac{2}{9} \left(C_{\epsilon 1} \frac{p}{\epsilon} - C_{\epsilon 2} \right). \quad (4.3)$$

Furthermore, we showed that the normalized dissipation can be expressed as a function of this perturbation, leading to the relation

$$\frac{C_\epsilon}{C_{\epsilon 0}} = \left(1 + \frac{\tilde{k}}{k} \right)^{-\frac{15}{14}}. \quad (4.4)$$

In the following we will use the $k - \epsilon$ model to compute k and ϵ , and we will determine the unsteady perturbation \tilde{k} *a posteriori*, using expression (4.3). This will allow us to estimate the non-equilibrium within the context of a two-equation turbulence model. We note here that this is possible in a 2-equation model, since we have access to the values of k , ϵ and $\dot{\epsilon}$. An even more reduced description, using only one equation (as for instance the model of Spalart & Allmaras, 1992) does not provide enough information on the turbulence to assess the imbalance in this way.

5. Results

5.1. Choice of the parameters

Equations (3.6-3.8) are integrated numerically in the high Reynolds number limit. The model constants are given their classical values (Jones & Launder, 1972) $C_{\epsilon 1} = 1.44$, $C_{\epsilon 2} = 1.92$ and $C_{\nu} = 0.09$. We have chosen initial conditions which are in the range of experimentally relevant values. To characterize the grid-spacing, we have chosen $M = 10\text{cm}$. The value of U is typically an order of magnitude smaller than the mean flow velocity, which is of order 10ms^{-1} . We have therefore set the average-field kinetic energy to $K = 1\text{m}^2\text{s}^{-2}$. The initial value of the fluctuating quantities k and ϵ are hard to estimate. Indeed, they depend on the precise instability mechanisms of the grid-bar-wakes and the incoming turbulence intensity. We have therefore proceeded by taking two different values for k . We define the turbulence intensity by

$$I_k = \frac{k}{K}. \quad (5.1)$$

Our first set of experiments corresponds to the intensity $I_k = 0.1$, the second one where the initial velocity fluctuations are an order of magnitude smaller than the mean-field amplitude, $I_k = 0.01$.

The initial values of ϵ are even harder to estimate. The variation of ϵ is in particular important, since for given k and M , it determines the initial lengthscale ratio $\alpha_L(0)$, defined in expression (3.12). The influence of this parameter on the dynamics constitutes one of the main issues of this investigation. Very large values of $\alpha_L(0)$ correspond to a strong transverse mixing of the turbulence near the grid as expected in active grids. Small initial values correspond to the case where the wakes are slowly perturbed by the developing turbulence, and the influence of the mean-flow, i.e. the wakes, is sensible far behind the grid. This corresponds to small initial turbulent intensity with a small initial lengthscale. Since the variation of this parameter is the key parameter in our study, we have varied it over three orders of magnitude, in the range $0.01 \leq \alpha_L(0) \leq 10$.

The initial values of I_k and α_L are the physical control parameters of our system. The numerical integration of three coupled ODEs is performed using an explicit Euler integration scheme. The conservation of energy was estimated by monitoring the sum of the integral of the dissipation and the total kinetic energy in the system. Timesteps were set to $\Delta t = 10^{-4}$. A typical simulation of the system upto $t = 100$ takes several seconds on a common desktop computer. More complicated numerics did not seem to be necessary.

5.2. Evolution of the kinetic energy and dissipation

In Figure 2(a,b) we show the evolution of the turbulent kinetic energy for both turbulence intensities we studied, and a wide range of values of $\alpha_L(0)$. Clearly, it is shown that the results are not very sensitive with respect to the choice of the initial turbulent intensity, at least for the values $I_k = 0.1$ and 0.01 which we considered. We further see that for long times the model behaves as expected, with a power law decay

$$k \sim t^{-n}, \quad (5.2)$$

where $n = 1/(C_{\epsilon 2} - 1) \approx 1.1$.

In Figure 2(c) the kinetic energy for $I_k = 0.01$ is replotted, normalized by its peak-value. Time is normalized by t_{peak} , the time at which the kinetic energy peaks. Around the peak, the time-dependence differs for the different cases. In particular it is observed that a very good agreement with experiments is obtained for values of $\alpha_L(0) \approx 0.3$. In this timespan the time-dependence of the kinetic energy can be approximated, for the

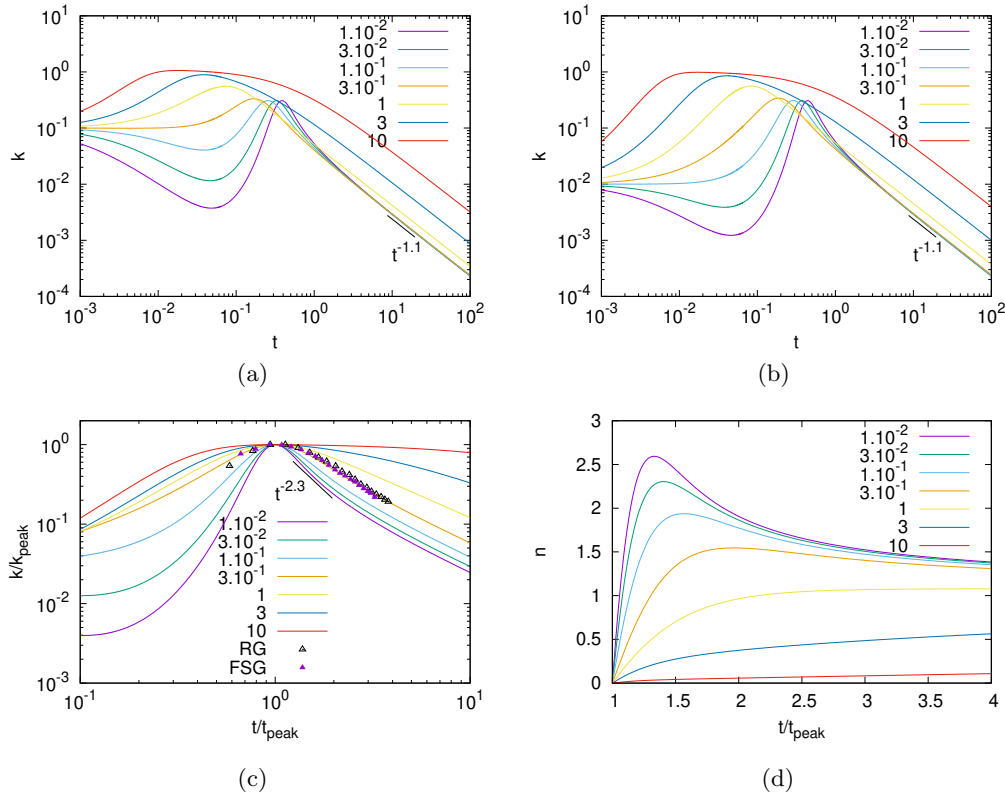


FIGURE 2. Temporal evolution of the kinetic energy of the turbulence for values of the lengthscale ratio $0.01 \leq \alpha_L(0) \leq 10$. (a) Initial intensity $I_k = 0.1$; (b) $I_k = 0.01$. (c) Same results as in (b) but time is normalized by t_{peak} and kinetic energy by k_{peak} . Also shown is a comparison with data obtained from a Fractal Square Grid (FSG) and a Regular Square Grid (RG), data from Valente & Vassilicos, 2014. (d) Local power law decay exponent of the kinetic energy n .

smallest values of $\alpha_L(0)$, by a power law with an exponent $n \approx 2.3$, but this interval is too short to identify a true power law. The steeper-than-expected decay of kinetic turbulence seems rather to be due to a change in virtual origin than in a qualitative change of the physics. For a further discussion on the fitting of power law behaviour to the data and the choice of virtual origins we refer to the investigations of Mohamed & Larue, 1990 and Valente & Vassilicos, 2011. The local decay exponent, i.e., when the function is approximated by a power law, is

$$n = -\frac{d \log(k)}{d \log(t)}. \quad (5.3)$$

This exponent is plotted in figure 2(d). It is observed that in the *active grid* limit (large $\alpha_L(0)$), the decay exponent monotonically increases from $n = 0$ at the peak to $n \approx 1.1$ for long times. Only for small initial values of α_L an overshoot is observed with maximum values of the order of $n \approx 2.5$.

The mean-flow energy evolution is shown in figure 3(a). We observe, that irrespective of the parameters, the mean-energy decays rapidly, reducing its value by approximately 10 orders of magnitude in the interval $0 < t < 1$. It is thus in this interval that the influence of the production of kinetic energy by the shear-layer decreases from order unity to negligible. Clearly, it is this very fast decay of the mean field that makes grid-

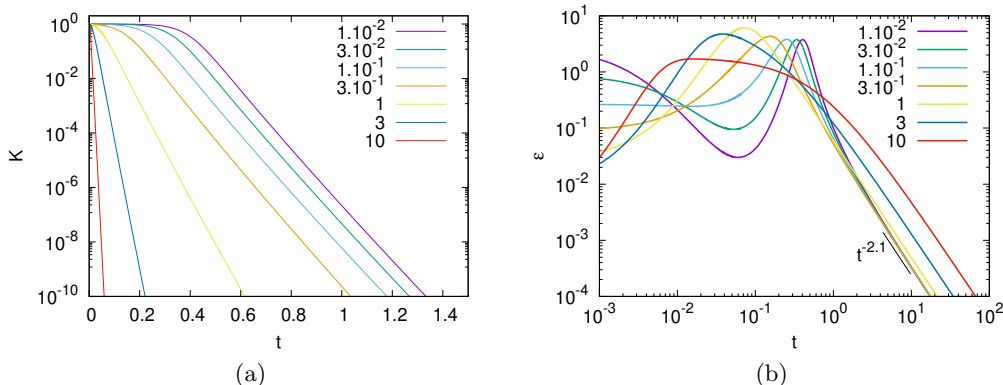


FIGURE 3. Temporal evolution of (a) the kinetic energy of the mean field and (b) the dissipation of the turbulence, for values of the lengthscale ratio $0.01 \leq \alpha_L(0) \leq 10$; initial intensity $I_k = 0.01$.

turbulence such a good candidate to study freely decaying isotropic turbulence. In the limit of large $\alpha_L(0)$, the kinetic energy of the mean field is thus rapidly absorbed by the turbulence. For this limit the flow should approach the freely decaying limit for which an analytical solution exists. For further discussion of this analytical solution we refer to appendix 2.

In Figure 3(b) we show the evolution of the dissipation of turbulent kinetic energy. The qualitative behaviour resembles that of the kinetic energy in most aspects. The overall shapes of the curves are similar. But since we fixed the initial value of k and varied the value of $\alpha_L(0)$, the initial values of ϵ are not the same for the different runs so that the peak values of the dissipation behave differently from those of the kinetic energy plotted in figure 2. For long times the expected power law, proportional to $t^{-(n+1)}$ is observed.

5.3. Nonequilibrium dissipation scaling

The equilibrium value of C_ϵ is obtained when the production is equal to the dissipation. Such a steady state, which is in addition isotropic is hard to obtain experimentally, but in numerical simulations, forced isotropic turbulence in a periodic domain is a canonical flow (Ishihara *et al.*, 2009). The exact value might depend on the type of forcing, but for a given flow, for increasing R_λ the value of $C_{\epsilon 0}$ tends to a constant value (Kaneda *et al.*, 2003). In freely decaying isotropic turbulence, the normalized dissipation rate, at high Reynolds numbers tends to a different constant value, which depends weakly on the initial conditions (Bos *et al.*, 2007). The reason for this is that in the case of decaying turbulence, where p goes to zero, the non-equilibrium will tend to an asymptotic value. The analytical prediction of this value is, according to equations (4.3) and (4.4),

$$\frac{C_\epsilon}{C_{\epsilon 0}} = \left(1 - \frac{2}{9}C_{\epsilon 2}\right)^{-\frac{15}{14}} \approx 1.8. \quad (5.4)$$

In figure 4 we show our estimate of $C_\epsilon/C_{\epsilon 0}$, as determined by (4.3) and (4.4). We have also compared to the data of Vassilicos, 2015, figure 4(b), where different data-sets produced from wind-tunnel measurement behind a fractal grid are reported. Since we do not exactly know how to match the initial conditions of the experiments with our simulations, our comparison will be at best qualitative. Therefore, we have collapsed the asymptotic long-time value of 1.8 with the experimental data, and we have shifted the data-points in time to get a best agreement. This will only assess whether the transient towards the

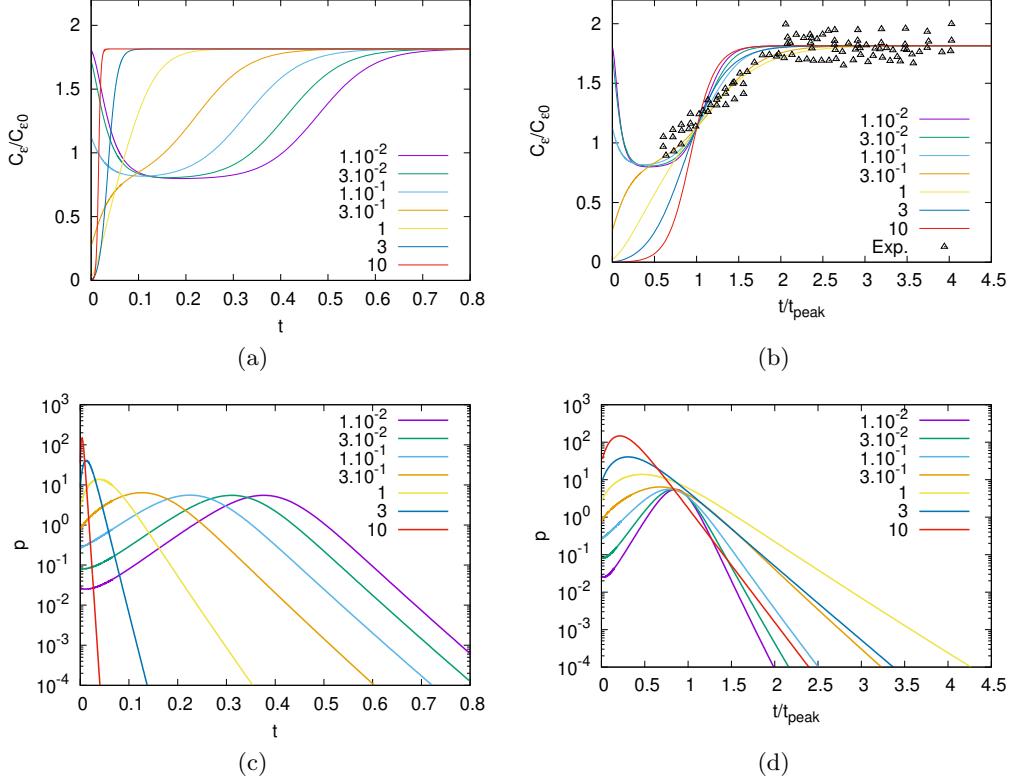


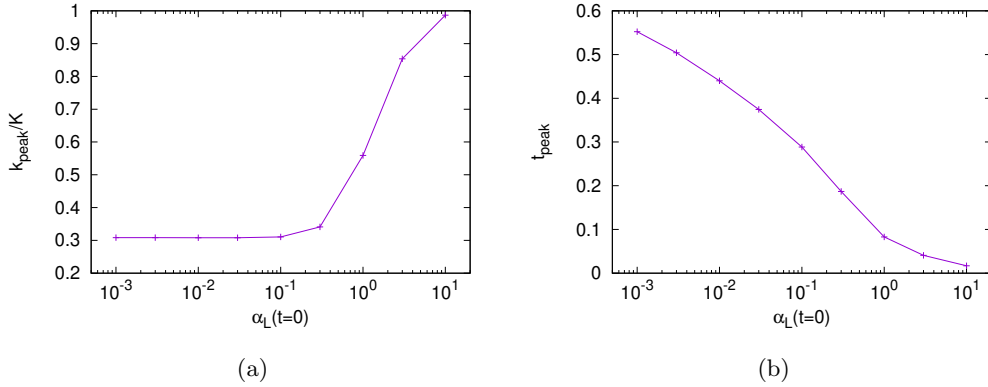
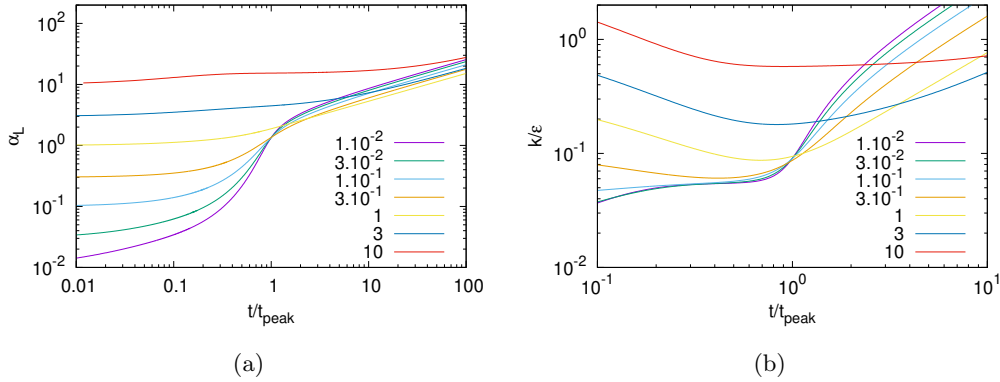
FIGURE 4. (a) Normalized dissipation rate for values of the lengthscale ratio $0.01 \leq \alpha_L(0) \leq 10$ and initial intensity $I_k = 0.01$. (b) Same results but with time normalized by t_{peak} , the time where the kinetic energy peaks. Also shown experimental data from Vassilicos, 2015. (c,d) The production of turbulent kinetic energy as a function of time, or normalized time.

self-similar decaying state in our model shows the same time-dependence as the one observed in the experiments, but will not assess the quantitative agreement.

Clearly, the behaviour of the experiments is qualitatively reproduced. Furthermore, the transition from a monotonically rising value of C_ϵ to a plateau-value is abrupt as in the experiments. The physical reason for this is the rapid decrease of the production term as observed in Figure 4(c,d). The production shows, as the mean-kinetic energy, a rapid decay at later times. The time at which this decay sets in is increasing with decreasing $\alpha_L(0)$.

5.4. Short-time evolution and determination of the peak-value of the kinetic energy.

In figure 5(a) we show how the peak of the kinetic energy of the turbulence depends on the parameter $\alpha_L(0)$. It is observed that for large values of $\alpha_L(0)$ almost all energy of the mean field K is converted in turbulent fluctuations. This corresponds to the case where the lengthscale of the turbulence is initially large, so that the mean field is immediately distorted by the turbulent fluctuations. This limit corresponds to active grid turbulence. When the initial fluctuations are initially very small, an asymptotic value of roughly 30% of the mean field energy is converted into turbulent fluctuations. The system seems to become independent on the size of the initial fluctuations for this limit. In figure 5(b) the location of the peak is determined. The quantity t_{peak} corresponds to the time-instant where the kinetic energy attains its peak value. Obviously, this value cannot become

FIGURE 5. Peak values of the kinetic energy for $0.001 \leq \alpha_L(0) \leq 10$ and $I_k = 0.01$.FIGURE 6. Temporal evolution of the turbulent timescale $\tau = k/\epsilon$ for $0.01 \leq \alpha_L(0) \leq 10$ and $I_k = 0.01$.

negative. It is observed that in the limit where all the mean field energy is converted into fluctuations, the peak is located very close to the grid. For decreasing values of $\alpha_L(0)$ this distance is located further downstream. We will now explain these observations.

From equation (3.6) we can deduce the typical time-scale over which the mean-flow evolves,

$$T = \left(\frac{1}{K} \frac{dK}{dt} \right)^{-1} = \frac{\epsilon \tilde{M}^2}{k^2}. \quad (5.5)$$

The typical timescale of the turbulence is $\tau \equiv k/\epsilon$. Comparing these timescales we find that in the limit

$$\frac{\tau}{T} = \frac{k^3}{\epsilon^2 \tilde{M}^2} \ll 1, \quad (5.6)$$

the mean flow evolves much slower than the turbulence. In this case the shear induced by the wakes can thus be treated as a steady shear. Note that this time-scale ratio is the square of the lengthscale ratio, α_L .

In figure 6(a) we show how α_L evolves. Clearly for small initial values of α_L , its value becomes of order unity approximately at $t = t_{peak}$, and before this time it is smaller. In the early times, the turbulent flow behaves thus as turbulence subjected to a steady

shear. The average value of this shear is according to expression (3.5),

$$S \sim \frac{K^{1/2}}{M}. \quad (5.7)$$

It is well known that the k - ϵ model applied to steady shear predicts exponential evolution of the kinetic energy and dissipation (Pope, 2000),

$$k \sim k^* \exp(St) \quad (5.8)$$

$$\epsilon \sim \epsilon^* \exp(St) \quad (5.9)$$

The values of k^* and ϵ^* are set by the asymptotic value of $S^* \equiv Sk^*/\epsilon^* \approx 3$. We can therefore estimate the time at which the shear-layers start to decay, by comparing

$$\frac{\tau}{T}|_{t=t_*} = \mathcal{O}(1) \quad (5.10)$$

we find that

$$t^* \sim \frac{1}{S} \ln \left(\frac{\tilde{M}^2 \epsilon^{*2}}{k^{*3}} \right). \quad (5.11)$$

In order to find the peak value of the turbulent kinetic energy, we determine $k(t^*)$ by combining (5.11) and (5.8). This yields

$$k(t^*) \sim \frac{\epsilon^{*2} \tilde{M}^2}{k^{*2}}, \quad (5.12)$$

which can be simplified to

$$k(t^*) \sim \frac{K(t=0)}{S_*^2}. \quad (5.13)$$

This shows that the peak of the turbulent kinetic energy corresponds to a fixed fraction of the total injected energy. In Figure 6(b), we show the evolution of the turbulent time-scale τ . It is observed that for sufficiently small initial values of $\alpha_L(0)$, τ is approximately constant for a short time-interval $0.2 < t_{peak} < 0.8$. It is in this region that exponential increase of the kinetic energy and dissipation (eqs. (5.8) and (5.9)) is simultaneously observed.

The short-time evolution of the energy budget of the system can thus be accurately described as homogeneous, steady shearflow and the asymptotic behaviour of this system sets the peak of the turbulent kinetic energy and the time instant where the peak occurs. This approximation is only valid for small initial values of $\alpha_L(0)$.

6. Concluding remarks

The main goal of this investigation was to obtain a better understanding of the influence of initial conditions on grid turbulence. In order to achieve this goal we have shown how to describe, statistically, the interaction of a mean field generated behind a grid with a spatially developing turbulent flow. The application of an eddy-viscosity model allowed to identify a parameter α_L , proportional to the ratio of the mesh-size to the integral lengthscale, which appears explicitly in the evolution equations of the energy budget. It is this α_L which is arguably large in active-grids, so that the influence of the initial conditions in turbulence generated by such grids is rapidly negligible. However for passive grids this parameter is smaller since the turbulence has to develop through the interaction with the shear layers. In such flows the influence of the initial conditions is expected to persist for longer time intervals.

The $k-\epsilon$ model turns out to be a convenient tool to understand and evaluate the energy budget in near-grid grid turbulence. That such a simple model can be so performant is due to several reasons. First of all, we consider integral quantities, such as the kinetic energy averaged over a period of the grid. This average allows to remove the influence of turbulent diffusion from our description. Secondly, the used model is known to give reasonable results for both shear flows and free decay. The present flow does not contain more complicated effects (mean swirl, rotation, pressure gradients, obstacles, ...) and is therefore easier to predict than flows which do contain such features.

These insights allow now to give answers to the questions which were raised in the introduction.

- The sudden transition from the power law evolution of C_ϵ to a constant value is caused by the rapid decay of the production term in this zone. The turbulence evolves here from a state where the production is equal or larger than the dissipation, to a state where the production becomes negligible.
- The downstream distance where this happens depends on the initial lengthscale ratio α_L . In particular, when this ratio is decreasing, the distance behind the grid where the kinetic energy peaks increases.
- For active grids this distance is arguably much smaller than for passive grids.
- The peak of the kinetic energy is naturally bounded by the total kinetic energy in the flow. The minimum fraction of the mean energy converted into turbulent kinetic energy tends to a constant of order 0.3 for small values of $\alpha_L(0)$.

We showed that in this latter limit, of small initial value of the lengthscale ratio, the time-dependence of the kinetic energy directly behind the peak of the kinetic energy is steeper than the asymptotic power law exponent, the opposite trend is observed for large values of $\alpha_L(0)$

We showed that the non-equilibrium, as quantified by the normalized dissipation, can be evaluated *a posteriori* from the results of the $k-\epsilon$ model. The next challenge is to use this estimate to improve the performance of the model in cases where the non-equilibrium deteriorates its performance. One application is the modeling of turbulent flow around obstacles, since the non-equilibrium affects the spreading of the radial extent of the wake (see for example Obligado *et al.*, 2016). This seems an excellent subject for further research.

Appendix 1: derivation of the equations for K and k .

We start from the incompressible Navier-Stokes equations,

$$\partial_t U_i + U_j \partial_j U_i = -\partial_i \Pi + \nu \partial_j^2 U_i, \quad (6.1)$$

and $\partial_i U_i = 0$. We decompose the flow into an ensemble averaged part and a fluctuating part $U_i = \bar{U}_i + u_i$ and the pressure divided by density is $\Pi = \bar{\Pi} + \pi$. The three components of the fluctuating velocity are indicated by $(u_1, u_2, u_3) = (u, v, w)$. Furthermore we consider the case where the mean flow is unidirectional, homogeneous in the x -direction and varying in only one direction y perpendicular to the flow direction x ,

$$\bar{U}_i = \bar{U}(y) \delta_{i1}. \quad (6.2)$$

For grid-turbulence this means that we are moving in a reference frame with constant velocity U_0 . The equation for the mean field then reads

$$\partial_t \bar{U} = -\partial_j \bar{u} \bar{u}_j + \nu \partial_y^2 \bar{U}. \quad (6.3)$$

The equation for the fluctuations reads,

$$\partial_t u_i + \bar{U} \partial_x u_i + v \partial_y \bar{U} \delta_{i1} = -\partial_j (\delta_{ij} \pi + u_i u_j) + \nu \partial_j^2 u_i, \quad (6.4)$$

so that the kinetic energy of the mean field and of the fluctuations obey

$$\frac{1}{2} \partial_t \bar{U}^2 = -\partial_j (\bar{U} \overline{u u_j}) + \overline{u v} \partial_y \bar{U} + \nu \partial_y^2 \left(\frac{1}{2} \bar{U}^2 \right) - \nu (\partial_y \bar{U})^2, \quad (6.5)$$

and

$$\frac{1}{2} \partial_t \overline{u_i u_i} + \frac{1}{2} \bar{U} \partial_x \overline{u_i u_i} + \overline{u v} \partial_y \bar{U} = -\partial_j \left(\delta_{ij} \overline{u_i \pi} + \frac{1}{2} \overline{u_i u_i u_j} \right) + \nu \partial_j^2 \left(\frac{1}{2} \overline{u_i u_i} \right) - \nu \overline{\partial_j u_i \partial_j u_i}, \quad (6.6)$$

The turbulence is considered statistically homogeneous in the x - and z -direction. All gradients of averaged quantities then vanish in these directions, leading to

$$\frac{1}{2} \partial_t \bar{U}^2 = -\partial_y (\bar{U} \overline{u v}) + \overline{u v} \partial_y \bar{U} + \nu \partial_y^2 \left(\frac{1}{2} \bar{U}^2 \right) - \nu (\partial_y \bar{U})^2, \quad (6.7)$$

and

$$\frac{1}{2} \partial_t \overline{u_i u_i} + \overline{u v} \partial_y \bar{U} = -\partial_y \left(\overline{v \pi} + \frac{1}{2} \overline{u_i u_i v} \right) + \nu \partial_y^2 \left(\frac{1}{2} \overline{u_i u_i} \right) - \nu \overline{\partial_j u_i \partial_j u_i}. \quad (6.8)$$

These equations give the precise, pointwise evolution of the kinetic energy of the flow with a cross-stream mean profile, in a reference frame moving with the mean-velocity. If we want to simplify, we have to know more on the mean-profile. In a periodic grid, of whatever type with a periodic spacing, the mean field will be periodic. Integrating the kinetic energy over one period, all terms which can be written as the gradient in the y -direction will cancel out. Defining the average kinetic energies,

$$K = \frac{1}{2M} \int_0^M \bar{U}^2 dy \quad (6.9)$$

$$k = \frac{1}{2M} \int_0^M \overline{u_i u_i} dy, \quad (6.10)$$

we have

$$\dot{K} = -p - D \quad (6.11)$$

and

$$\dot{k} = p - \epsilon \quad (6.12)$$

with

$$p = -\frac{1}{M} \int_0^M \overline{u v} \partial_y \bar{U} dy \quad (6.13)$$

$$\epsilon = \frac{\nu}{M} \int_0^M \overline{\partial_j u_i \partial_j u_i} dy \quad (6.14)$$

$$D = \frac{\nu}{M} \int_0^M (\partial_y \bar{U})^2 dy. \quad (6.15)$$

Equations (6.11) and (6.12) are thus exact for flows with a mean flow which is unidirectional and homogeneous in the streamwise direction and with a transverse periodic variation.

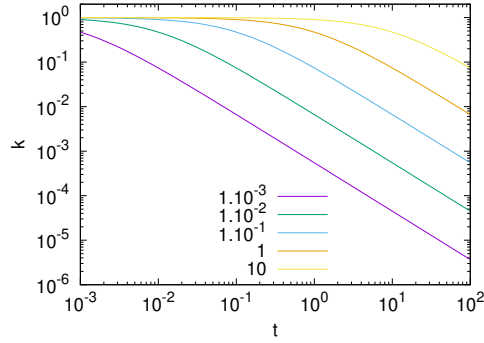


FIGURE 7. Analytical solution for the temporal evolution of the turbulent kinetic energy for freely decaying turbulence for different initial values of the ratio $t_0 = k(0)/\epsilon(0)$.

Appendix 2: Analytical solution for the kinetic energy in the active grid limit

The total energy of the flow, corresponding to both the fluctuating energy plus the mean field does not have a source term once the flow has passed the grid. Indeed, summing equations (6.11) and (6.12), the overall budget is evolving according to,

$$\dot{K}_{tot} = -\epsilon_{tot}. \quad (6.1)$$

where $K_{tot} = K + k$ and $\epsilon_{tot} = D + \epsilon$. In principle, in the present investigation D can be neglected compared to ϵ . The $k - \epsilon$ model reduces now to

$$\dot{K}_{tot} = -\epsilon \quad (6.2)$$

$$\dot{\epsilon} = -C_{\epsilon 2} \frac{\epsilon^2}{k}. \quad (6.3)$$

This system is not closed, and in the present investigation we have modeled the repartition of energy between K and k . Let us now consider the limiting case, which was identified for $\alpha_L(0) \gg 1$. In this case, which we coined the *active grid* limit, the energy is almost immediately transferred to the turbulence such that $K_{tot} \approx k$. For this case the above system has an analytical solution

$$\frac{k}{k(0)} = \left(\frac{t + t_0}{t_0} \right)^{-n} \quad (6.4)$$

with $n = 1/(C_{\epsilon 2} - 1)$ and $t_0 = nk(0)/(\epsilon(0))$. This expression is plotted in figure 7, for different values of t_0 .

REFERENCES

- BATCHELOR, G.K. & TOWNSEND, A.A. 1948. Decay of isotropic turbulence in the initial period. *Proc. R. Soc. Lond. A*, 193(1035), 539–558.
- BOS, W.J.T. & RUBINSTEIN, R. 2017. Dissipation in unsteady turbulence. *Phys. Rev. Fluids*, 2, 022601(R).
- BOS, W. J. T. , SHAO, L. , & BERTOGGIO, J.-P. 2007. Spectral imbalance and the normalized dissipation rate of turbulence. *Phys. Fluids*, 19, 045101.
- DISCETTI, S. , ZISKIN, I. B. , ASTARITA, T. , ADRIAN, R.J. , & PRESTRIDGE, K. P 2013. PIV measurements of anisotropy and inhomogeneity in decaying fractal generated turbulence. *Fluid Dyn. Res.*, 45(6), 061401.

- GEORGE, W.K. 1992. The decay of homogeneous isotropic turbulence. *Phys. Fluids A*, 4, 1492–1509.
- ISHIHARA, T. , GOTOH, T. , & KANEDA, Y. 2009. Study of high Reynolds number isotropic turbulence by Direct Numerical Simulation. *Annu. Rev. Fluid Mech.*, 41, 65.
- JONES, WP & LAUNDER, B.E. 1972. The prediction of laminarization with a two-equation model of turbulence. *International journal of heat and mass transfer*, 15(2), 301–314.
- KANEDA, Y. , ISHIHARA, T. , YOKOKAWA, M. , ITAKURA, K. , & UNO, A. 2003. Energy dissipation rate and energy spectrum in high resolution direct numerical simulations of turbulence in a periodic box. *Phys. Fluids*, 15(L21).
- KROGSTAD, P-Å & DAVIDSON, PA 2011. Freely decaying, homogeneous turbulence generated by multi-scale grids. *Journal of Fluid Mechanics*, 680, 417–434.
- MAKITA, H 1991. Realization of a large-scale turbulence field in a small wind tunnel. *Fluid Dynamics Research*, 8(1-4), 53.
- MELDI, M. & SAGAUT, P. 2018. Investigation of anomalous very fast decay regimes in homogeneous isotropic turbulence. *Journal of Turbulence*, 19(5), 390–413.
- MOHAMED, M.S. & LARUE, J.C 1990. The decay power law in grid-generated turbulence. *Journal of Fluid Mechanics*, 219, 195–214.
- MYDLARSKI, L. & WARHAFT, Z. 1996. On the onset of high-Reynolds-number grid-generated wind tunnel turbulence. *J. Fluid Mech.*, 320, 331.
- NAGATA, K. , SAKAI, Y. , INABA, T. , SUZUKI, H. , TERASHIMA, O. , & SUZUKI, H. 2013. Turbulence structure and turbulence kinetic energy transport in multiscale/fractal-generated turbulence. *Phys. Fluids*, 25(6), 065102.
- OBLIGADO, M. , DAIRAY, T , & VASSILICOS, JC 2016. Nonequilibrium scalings of turbulent wakes. *Physical Review Fluids*, 1(4), 044409.
- POPE, S.B. 2000. *Turbulent Flows*. Cambridge University Press.
- REYNOLDS, O. 1895. IV. On the dynamical theory of incompressible viscous fluids and the determination of the criterion. *Phil. Trans. Roy. Soc London.(a.)*, (186), 123–164.
- SIMMONS, L. F. G. & SALTER, C. 1934. Experimental investigation and analysis of the velocity variations in turbulent flow. *Proc. Roy. Soc. London A*, 145(854), 212–234.
- SPALART, PRAA & ALLMARAS, S1 1992. A one-equation turbulence model for aerodynamic flows. In *30th aerospace sciences meeting and exhibit*, page 439.
- TAYLOR, G.I. 1935. Statistical theory of turbulence. *Proc. Roy. Soc. London. Ser. A, Math. Phys. Sci.*, 151, 421–444.
- TENNEKES, H. & LUMLEY, J.L. 1972. *A first course in turbulence*. The MIT Press.
- THORMANN, A. & MENEVEAU, C. 2014. Decay of homogeneous, nearly isotropic turbulence behind active fractal grids. *Physics of Fluids*, 26(2), 025112.
- VALENTE, PC & VASSILICOS, J.C. 2011. The decay of turbulence generated by a class of multiscale grids. *Journal of Fluid Mechanics*, 687, 300–340.
- VALENTE, P.C. & VASSILICOS, J.C. 2014. The non-equilibrium region of grid-generated decaying turbulence. *J. Fluid Mech.*, 744, 5–37.
- VASSILICOS, J.C. 2015. Dissipation in turbulent flows. *Ann. Rev. Fluid Mech.*, 47, 95–114.